Chemistry & Biology, Vol. 12, 643–648, June, 2005, ©2005 Elsevier Ltd All rights reserved. DOI 10.1016/j.chembiol.2005.04.016

Dissecting RNA-Interference Pathway with Small Molecules

Brief Communication

Ya-Lin Chiu,[1] Chimmanamada U. Dinesh,[2] Chia-ying Chu, Akbar Ali, Kirk M. Brown, Hong Cao, and Tariq M. Rana*
Department of Biochemistry and Molecular Pharmacology
University of Massachusetts Medical School
Worcester, Massachusetts 01605

Summary

RNA interference (RNAi) is a process whereby short-interfering RNAs (siRNA) silence gene expression in a sequence-specific manner. We have screened a chemical library of substituted dihydropteridinones and identified a nontoxic, cell permeable, and reversible inhibitor of the RNAi pathway in human cells. Biochemical and fluorescence resonance-energy transfer experiments demonstrated that one of the compounds, named ATPA-18, inhibited siRNA unwinding that occurred within 6 hr of siRNA transfection. Extracts prepared from ATPA-18-treated cells also exhibited a decrease in target RNA cleavage by activated RNA-induced silencing complex (RISC*). Interestingly, when activated RISC*, which harbors unwound antisense siRNA, was treated with ATPA-18 in vitro, target RNA cleavage was not affected, indicating that this compound inhibited siRNA unwinding or steps upstream of unwinding in the RNAi pathway. Our results also establish the timing of siRNA unwinding and show that siRNA helicase activity is required for RNAi. ATPA-18 analogs will therefore provide a new class of small molecules for studying RNAi mechanisms in a variety of model organisms and deciphering in vivo genetic functions through reverse genetics.

Introduction

RNA interference (RNAi), the process by which mRNA is targeted for degradation by 21–23 nucleotide short-interfering RNA (siRNA), has become key to establishing connections between gene structure and function in human cells by reverse genetics (reviewed in [1, 2]). Because of its broad applications in biology and medicine, understanding the fundamental mechanism of RNAi phenomenon is of great importance. The current model for how RNAi occurs in vivo is shown in Figure 1A. In the first step of RNAi induction, the 5′ ends of the siRNA duplex are phosphorylated, resulting in the formation of an RNA-induced silencing complex (RISC)-siRNA complex [3, 4]. Additional ATP-dependent events take place next involving siRNA unwinding from the 5′ end of the antisense strand and activation of RISC (RISC*) [5]. After siRNA-programmed RISC* (siRISC*) activation, the antisense strand of the unwound siRNA guides the siRISC* complex to the target mRNA [6, 7]. The guide antisense-strand base pairs with the target mRNA, forming an A-form helical geometry recognized by RISC* [3, 8]. In the final step, RISC* cleaves the target mRNA [9]. RISC* can then be recycled to cleave another mRNA [10].

Recently, structural and biochemical studies defined Ago2 as the catalytic engine of RISC* that mediates the cleavage of the target RNA in human cells [11–13]. Other components of RISC required for RNAi have remained elusive, including the putative RNA helicase involved in unwinding siRNA. To identify new components of the RNAi pathway, we developed a screen for small molecules that block ATP-dependent steps of RNAi. Two small molecules identified in this screen were further characterized and were shown to specifically inhibit an early step in the RNAi pathway.

Results and Discussion

We took a small-molecule-based approach to dissect the ATP-dependent steps of the RNAi pathway. We synthesized a small chemical library of substituted dihydropteridinones as ATP analogs that contain both rigid and flexible scaffolds (C.U.D. and T.M.R., unpublished data) and screened their activities in a dual-fluorescence assay for RNAi induction [3]. In this assay, plasmids harboring enhanced green- and red-fluorescent proteins (EGFP and RFP, respectively) were cotransfected into HeLa cells with EGFP siRNA that targets EGFP mRNA for degradation. The ratio of EGFP/RFP fluorescence in the presence of siRNA was calculated and normalized to the EGFP/RFP ratio of mock treated cells. RNAi activity was then compared to RNAi in cells transfected with EGFP siRNA and treated with an ATP analog from the dihydropteridinones library. The screen was designed to identify small molecule probes that would specifically inhibit ATP-dependent events occurring during RNAi and, in doing so, inhibit RNAi. We identified two nontoxic compounds that showed concentration-dependent inhibition of RNAi in the dual-fluorescence assay. The structure of these compounds, designated ATPA-18 and ATPA-21, and their associated inhibitory activities are shown in Figure 1B.

To investigate whether ATPA-18 and ATPA-21 can inhibit RNAi against endogeneously expressed mRNA, we tested their effect on RNAi targeted to human CDK9 mRNA. CDK9 is the cyclin-dependent kinase component of the P-TEFb, CDK9-cyclinT1 complex, which is involved in regulating transcription elongation [14]. CDK9 double-stranded siRNA wholly complementary to CDK9 mRNA knocked down CDK9 protein levels substantially, unlike mock or mismatched CDK9 siRNA-treated cells (Figure 1C, lanes 1, 2, 7, 8 and 9). However, in the presence of increasing amounts of either ATPA-18 or ATPA-21 up to 100 μM, CDK9 protein levels were restored to normal, endogenous levels in a dose-

*Correspondence: tariq.rana@umassmed.edu
[1]Present address: Gladstone Institute of Virology and Immunology, University of California, San Francisco, California 94143.
[2]Present address: Synta Pharmaceuticals, Corp., 45 Hartwell Avenue, Lexington, Massachusetts 02421.

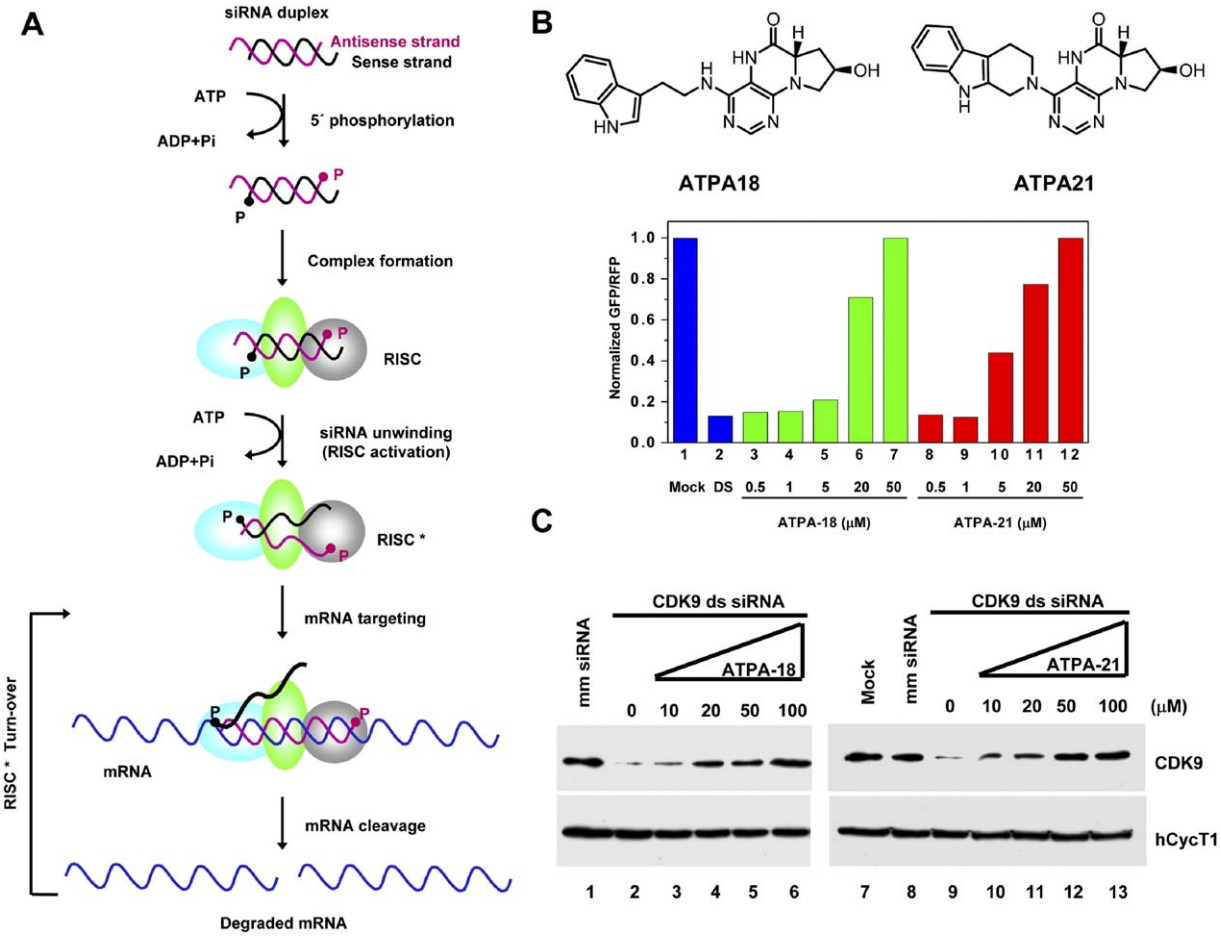

Figure 1. Small-Molecule Inhibitors of RNA Interference in Human Cells

(A) Model for RNAi in human cells highlighting the requirement of ATP.

(B) ATPA-18 and ATPA-21 as inhibitors of RNA interference in human cells. RNAi activity was quantified by the dual-fluorescence assay [3] and presented as the inhibition efficiency of target gene (EGFP) expression when cells were treated with 25 nM duplex siRNAs (DS) and small molecule inhibitors at 0.5–50 μM. Structures of the ATPA-18 and ATPA-21 exhibiting inhibition effects on RNAi are shown here.

(C) Effect of ATPA-18 and ATPA-21 on RNAi targeted to an endogenously expressed gene product. 150 nM CDK9 siRNA [14] were transfected into HeLa cells with or without inhibitor. At 42 hr posttransfection, proteins in 60 μg of total cell lysate were resolved by 10% SDS-PAGE, transferred onto polyvinylidene difluoride membrane (PVDF membrane, Bio-Rad), and probed with antibodies against CDK9 (Santa Cruz). As a loading control, the same membrane was also probed with anti-hCycT1 antibody (Santa Cruz). Protein contents were visualized with BM Chemiluminescence Blotting Kit (Roche Molecular Biochemicals). Immunoblots were exposed to X-ray film (Kodak MR-1) for various times (between 30 s and 5 min).

dependent manner (Figure 1C, lanes 3–6 and 10–13). These results suggested that the ATPA compounds generally interfered with RNAi regardless of whether mRNAs were expressed episomally or endogenously, and the degree of potency depended on the concentration of the ATPA.

We next examined the mechanism of how ATPA-18 and ATPA-21 induced their effects in vivo. One striking observation was that both ATPA compounds were unable to inhibit RNAi if cells were treated 6 hr after transfection (compare blue bars to red bars in Figure 2A). This finding established that the timing of the step(s) of the RNAi pathway affected by ATPA-18 and ATPA-21 occurred between 0–6 hr posttransfection. Because both compounds were showing identical effects, we chose to further characterize ATPA-18 in our studies.

First, localization patterns of siRNA were determined in the presence and absence of 100 μM ATPA-18. In the absence of ATPA-18, siRNA localized to areas surrounding the nucleus, and no significant differences in this localization were observed in the presence of ATPA-18 (Figure 2B). This suggested that ATPA-18 did not disrupt the cytoplasmic localization of siRNA [15–17].

The 5′ phosphorylation state and the single-stranded versus double-stranded nature of siRNA treated with the ATPA-18 were analyzed to determine how ATPA-18 was affecting the phosphorylation state and duplex structure of siRNA. In this particular assay, the siRNA antisense strands were biotinylated on their 3′ end (designated AS-3′-Biotin) because this end is not required for RNAi [3, 6, 18]. The mobility of siRNAs was established on a 20% polyacrylamide-7 M urea gel. When isolated in

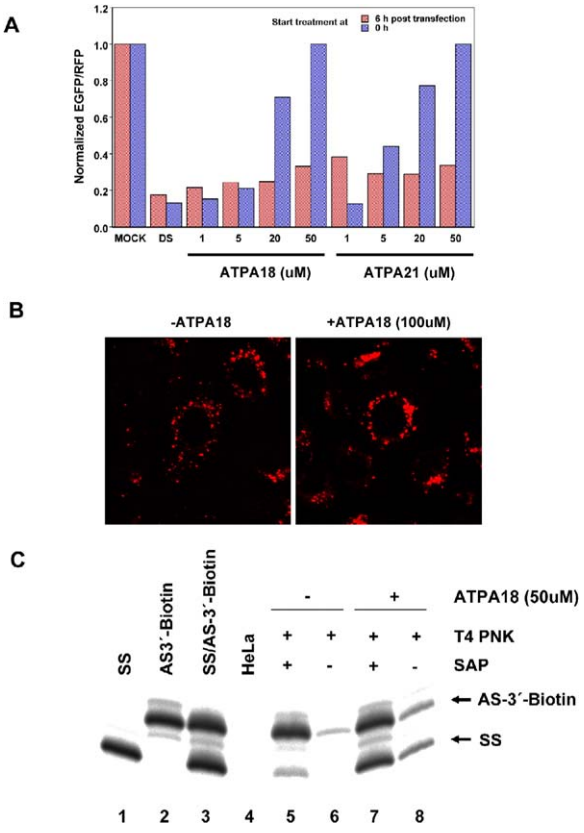

Figure 2. Cellular Target for Small-Molecule Inhibitors of RNA Interference in Human Cells

(A) ATPA-18 and ATPA-21 affected the step(s) of the RNAi pathway occurring between 0–6 hr posttransfection. RNAi activity was quantified by the dual-fluorescence assay and presented as the inhibition efficiency of target gene (EGFP) expression [3]. Cells were treated with 25 nM duplex siRNAs, and increasing concentrations of ATPA-18 and ATPA-21 were added at the beginning of transfection (0 hr, blue bar) or at 6 hr posttransfection (red bar).

(B) Localization patterns of siRNAs were not changed by ATPA-18. SS/AS-Alexa 568 duplex siRNAs with Alexa 568 labeling at the antisense strand 3′ terminus were transfected into HeLa cells, and the distribution pattern was determined in the presence and absence of 100 μM ATPA-18 at 6 hr posttransfection.

(C) Biotin pull-out assay indicating that helicase activity and not kinase activity was the cellular target for small-molecule inhibitors of RNAi in human cells. siRNA antisense strands were biotinylated on their 3′ end (designated AS-3′-Biotin). HeLa cells were cotransfected with biotinylated EGFP duplex siRNA (SS/AS3′-Biotin) and pEGFP-C1. siRNAs were isolated by streptavidin-magnetic beads and then were subjected to phosphatase and kinase reactions. Lanes 1–3 (marker lanes) contain 5′-end-labeled RNA sense strands (ss) (lane 1), 3′-biotinylated antisense strands (AS3′-Biotin) (lane 2), and heat-denatured (10 min at 95°C) siRNA duplexes (SS/AS3′-Biotin) (lane 3). Isolated biotinylated siRNA are shown with (lanes 5 and 7) or without SAP treatment (lanes 6 and 8). RNA isolated as above from HeLa cells without siRNA transfection is shown in lane 4.

a duplex form, the sense strand and the AS-3′-Biotin strands appeared as two distinct bands in the same lane (Figure 2C, lanes 1–3). Streptavidin magnetic beads were used to pull out biotinylated siRNAs from cells 6 hr posttransfection, washed to remove unbound RNA, and then split into two aliquots to determine if the 5′ end of the antisense strand was being phosphorylated. One aliquot was dephosphorylated with shrimp alkaline phosphatase (SAP) and the siRNA 5′ ends were labeled with ^{32}P by T4 polynucleotide kinase (PNK) reactions. The other aliquot was subjected to 5′-end radiolabeling by PNK without prior dephosphorylation by SAP. Cells that were not transfected with siRNA did not show any bands (Figure 2C, lane 4), indicating that the siRNAs recovered were specific to those transfected into cells and pulled out with streptavidin magnetic beads. In the absence of ATPA-18, efficient 5′ end radiolabeling was observed only when siRNA was pretreated with SAP. This indicated that the 5′ ends had been phosphorylated in vivo (Figure 2C, lanes 5 and 6), thereby preventing the addition of a phosphate group without prior removal of the phosphate group added in vivo. In addition, predominantly only the biotinylated antisense strands were pulled out from cells in the absence of ATPA-18. These results indicated that recovered siRNAs were mostly single stranded, signifying that the duplex had been unwound prior to removal from cells.

In the presence of 50 μM ATPA-18, which was added at the time of transfection, efficient 5′-end radiolabeling was observed only when siRNA was pretreated with SAP (Figure 2C, lanes 7 and 8), indicating that the 5′ ends had been phosphorylated in vivo, as was seen in the absence of ATPA-18. This strongly suggested that ATPA-18 was not blocking the siRNA 5′ phosphorylation step of the RNAi pathway. However, in contrast to what was observed in the absence of ATPA-18, a significant amount of sense strand siRNA was pulled out with the biotinylated antisense strand upon treatment with ATPA-18 (Figure 2C, lanes 7 and 8 arrows). The presence of both strands signified that the siRNA duplex had not been efficiently unwound at the time AS-3′-Biotin was recovered from the cell. This result demonstrated that the ATPA-18 analog was specifically affecting the unwinding step of the RNAi pathway, suggesting that the target of ATPA-18 inhibition was an ATP-dependent RNA helicase.

To directly study the effects of ATPA-18 on siRNA unwinding in vivo, we designed fluorescence resonance energy transfer (FRET) experiments to distinguish wound and unwound siRNA. FRET, in which a fluorescent donor molecule transfers energy via a nonradiative dipole-dipole interaction to an acceptor molecule [19], is a powerful spectroscopic technique for visualizing the phenomenon associated with the distance change between donors and acceptors. The efficiency of FRET (E_{FRET}) can be expressed as equation 1:

$$E_{FRET} = \frac{R_0^6}{R_0^6 + R^6} \quad (1)$$

in which R is the distance between donor and acceptor, and R_0 is the Förster distance. Practically, E_{FRET} can be calculated by measuring the donor fluorescence intensity in the absence of an acceptor (I_D) and in the presence of an acceptor (I_{DA}) (equation 2).

$$E_{FRET} = 1 - \frac{I_{DA}}{I_D} \quad (2)$$

In this work, Alexa Fluor 568 (donor) was conjugated

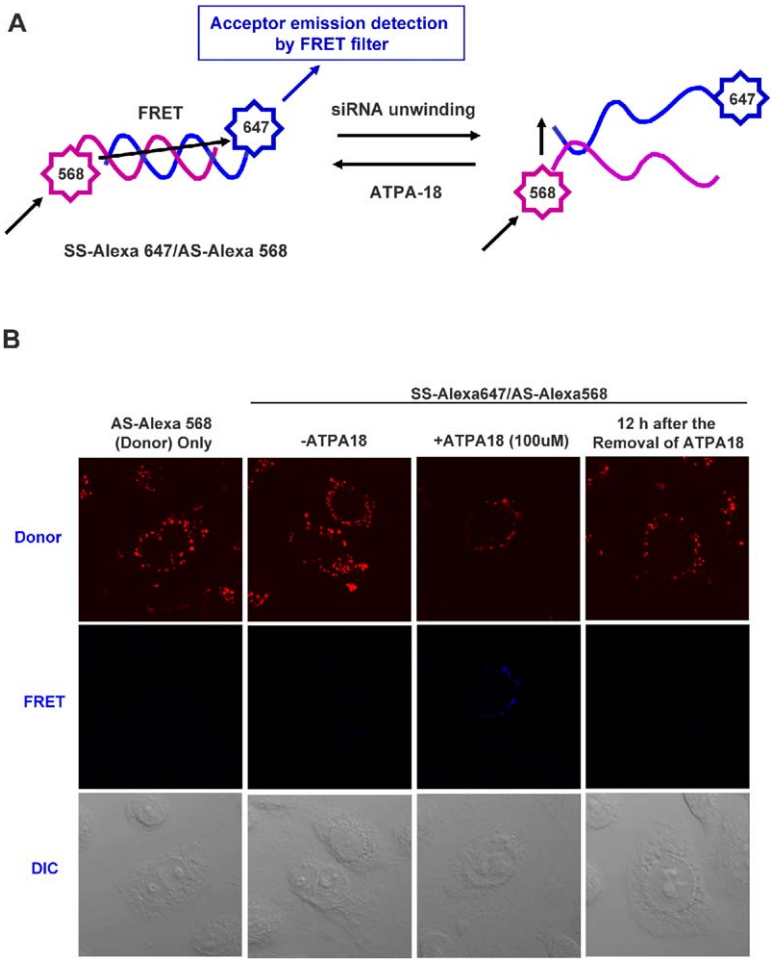

Figure 3. Effect of ATPA-18 on siRNA Unwinding In Vivo

siRNA were labeled with Alexa 647 and Alexa 568 at the 3′ terminus of the siRNA sense and antisense strand, respectively. Duplex siRNA (SS-Alexa 647/AS-Alexa 568) were transfected into HeLa cells with or without ATPA-18 treatment. Transfection mixtures were removed at 6 hr posttransfection, and cells were continuously cultured in the presence or absence of ATPA-18. Cells were imaged at 8 hr posttransfection. Cells were imaged with a Leica confocal imaging system (TCS-SP2) attached to a Leica DMIRE inverted fluorescence microscope and equipped with an acousto-optic tunable filter (AOTF) and a tunable acousto-optical beam splitter (AOBS). A 63×, 1.32 NA oil-immersion objective was employed. For donor (AS-Alexa 568) detection, the fluorescence emission signal was recorded at 585 ± 30 nm when excited at the Alexa 568 excitation wavelength (543 nm). For FRET signal detection, the fluorescence emission signal was recorded at 675 ± 25 nm when excited at the Alexa 568 excitation wavelength (543 nm).

to the antisense siRNA (AS-Alexa 568) and Alexa Fluor 647 (acceptor) labeled the sense siRNA (SS-Alexa 647). Both donor and acceptor were conjugated at the 3′-end of each strand (Figure 3). FRET would only be observed when the labeled siRNA was in a duplex structure, and would not be observed when siRNA was unwound (Figure 3A), providing an unambiguous method of analyzing RNA helicase activity.

We observed fluorescence with the donor filter and not the FRET filter when only AS-Alexa 568 was transfected into cells (Figure 3B, left). FRET was not observed when AS-Alexa 568/SS-Alexa 647 siRNA was transfected into HeLa cells in the absence of ATPA-18 (Figure 3B, second panel from left), indicating that siRNA unwinding had occurred. In the presence of ATPA-18, fluorescence was observed with both the donor and FRET filters. This indicated that unwinding had not occurred and that ATPA-18 specifically inhibited siRNA unwinding in vivo, corroborating the above biotin pull-out analysis that showed siRNA in ATPA-18-treated cells did not unwind at a high efficiency. The inhibitory effect of ATPA-18 on siRNA unwinding was reversible because FRET was lost when ATPA-18 was removed from the cell media for 12 hr, signifying that the RNA helicase had regained the capacity to unwind siRNA. This loss of FRET is not likely due to siRNA degradation because we observed RNAi over a period of 54 hr after removal of ATPA-18 (data not shown).

Another approach for detecting FRET in siRNA was utilized in which donor emission lost by energy transfer during FRET was restored by deliberately photobleaching the acceptor fluorophore, abolishing its capacity as an energy acceptor, to quantitatively determine the E_{FRET} in vivo between AS-Alexa 568 and SS-Alexa 647 [20, 21]. Unwound siRNA gives a very small E_{FRET}, and photobleaching of the Alexa 647 would not affect the fluorescence of Alexa 568. If ATPA-18 inhibits siRNA unwinding and FRET between Alexa 568 and Alexa 647 occurs, photobleaching would result in an increment of Alexa 568 fluorescence intensity (Figure S1A available with this article online), and a high E_{FRET} would be obtained.

In the absence of ATPA-18, acceptor emissions were not detected, and a change in donor fluorescence was not detected after acceptor photobleaching (data not shown), indicating that FRET had not occurred and unwinding had taken place. In the presence of ATPA-18, prior to acceptor photobleaching, the donor showed weak fluorescence, whereas the acceptor displayed strong fluorescence signals (Figure S1B, panels 1 and 2). After photobleaching, donor fluorescence became quite strong, acceptor fluorescence was no longer observed, and photobleaching efficiency was 94.8% (Figure S1B, panels 3 and 4). The energy transfer efficiency was calculated to be 77.9%. These results indicated that FRET occurred between AS-Alexa 568 and SS-Alexa

647 and strongly suggested that unwinding had not occurred in the presence of ATPA-18.

To determine if ATPA-18 effects were specific to double-stranded siRNA, we measured RISC* activity in the presence and absence of ATPA-18 in vitro. In these experiments, duplex siRNA was transfected into cells, cells were harvested 24 hr post transfection, and the extracts prepared from these transfected cells were incubated with ^{32}P-labeled target RNA in an in vitro cleavage reaction [22, 23]. The cell extracts contain GFP siRNA or *let-7* microRNA (miRNA), which is a 21–22 nt endogenous RNA that associates with RISC to inhibit translation. The effect of ATPA-18 on RISC* activity was measured by comparing target cleavage efficiency observed in untreated in vitro cleavage reactions to the cleavage efficiency seen when ATPA-18 was added to reactions at increasing concentrations. Note that the effect of ATPA-18 on RISC* in these extracts would be specific to single-stranded and not double-stranded siRNA or miRNA because both RNAs were unwound in vivo prior to harvesting. Neither siRNA- nor miRNA-programmed RISC* activity were affected by the addition of ATPA-18 (Figure S2A), suggesting that single-stranded siRNA or miRNA complexed with RISC* was not sensitive to this inhibitor. To test the effect of ATPA-18 on target RNA cleavage prior to unwinding, we transfected cells with siRNA and treated cells with or without ATPA-18. Cell extracts were prepared, and in vitro cleavage reactions were performed as described above. Extracts from cells that were not treated with ATPA-18 showed ~40% cleavage, whereas extracts from cells treated with ATPA-18 showed ~18% cleavage (Figure S2B), suggesting that ATPA-18 was affecting an early step in the RNAi pathway that occurred at the step of or prior to siRNA unwinding. *let-7*-programmed RISC* was not affected by ATPA-18 in these experiments (Figure S2B). Presumably, endogenous *let-7* miRNA was already unwound and associated with activated RISC* prior to ATPA-18 treatment and, thus, was not affected by an inhibitor of early steps in the RNAi pathway.

Our experiments identified nontoxic, cell-permeable, fast-acting, and reversible small molecules that modulate the RNA-interference pathway in human cells. This reversibility provides a new strategy for modulating reverse genetics by using small molecules and RNAi to exploit the control of gene expression and evaluate the effects of gene knockdown. ATPA-18 was further characterized as a potent, targeted inhibitor of a discrete step of the RNAi pathway in human cells, and our results raise the possibility that ATPA-18 may inhibit a specific ATP-dependent RNA helicase in human cells during RNAi. This analysis of ATPA-18 showed that a small molecule could be used to specifically inhibit an early step in the RNAi pathway, which may include siRNA entry into the pathway, RISC loading, and/or siRNA unwinding. Our results also demonstrated in vivo that events occurring prior to or at the step of siRNA unwinding are ATP dependent and essential for RNAi induction. Our studies also established the timing of siRNA unwinding to be within the first 6 hr of transfection. However, once unwinding occurs within 6 hr of siRNA transfection, RNAi cannot be inhibited by ATPA-18, indicating that the unwinding step was not reversible once completed. With the importance of these early steps in the RNAi pathway and unwinding now established in vivo, current studies are focused on isolating the ATP-dependent target of ATPA-18 and characterizing its role in the RNAi pathway. Comparing the effects of these inhibitors on the RNAi pathway in other model organisms will also be interesting to study in the future.

Significance

During RNA interference (RNAi), a double-stranded small-interfering RNA (siRNA) in association with the RNA-induced silencing complex (RISC) targets a complementary mRNA for site-specific cleavage and subsequent degradation. An 21–22 nucleotide siRNA duplex is loaded onto the RISC complex, the siRNA duplex is unwound, and RISC is activated (RISC*) to induce RNAi in human cells. Upon recognizing complementary mRNA, RISC* (siRISC*) specifically interacts with the target mRNA and cleaves the mRNA at a single site. To identify new components of the RNAi pathway, we screened a chemical library of substituted dihydropteridinones for small molecules that specifically inhibit RNAi in human cells. From this screen, a nontoxic, cell-permeable, and reversible inhibitor of the RNAi pathway was identified. This compound, called ATPA-18, specifically inhibited an early step in the RNAi pathway that occurred within 6 hr of siRNA transfection. These early steps may include siRNA entry into the RNAi pathways, RISC loading, and/or siRNA unwinding. ATPA-18 effects were specific to double-stranded siRNA, and RISC* was not inhibited when treated with ATPA-18 after unwinding has occurred. These results demonstrate that the early steps of RNAi, including siRNA unwinding, are essential for inducing RNAi, and our findings establish that siRNA is unwound in cells during a specific span of time. Taken altogether, ATPA-18 analogs represent a new class of small molecules that should prove useful for studying RNAi mechanisms and new gene functions in vivo in a variety of model organisms.

Supplemental Data

Supplemental Data include two figures and can be found with this article online at http://www.chembiol.com/cgi/content/full/12/6/643/DC1/.

Acknowledgments

We thank members of the Rana Lab for helpful discussions and Tamara J. Richman for editorial assistance. This work was supported in part by grants from the National Institutes of Health (AI 41404 and AI 43198) to T.M.R.

Received: December 22, 2004
Revised: April 19, 2005
Accepted: April 19, 2005
Published: June 24, 2005

References

1. Hannon, G.J. (2002). RNA interference. Nature *418*, 244–251.
2. Meister, G., and Tuschl, T. (2004). Mechanisms of gene silencing by double-stranded RNA. Nature *431*, 343–349.
3. Chiu, Y.L., and Rana, T.M. (2002). RNAi in human cells: basic

structural and functional features of small interfering RNA. Mol. Cell *10*, 549–561.

4. Hammond, S.M., Bernstein, E., Beach, D., and Hannon, G.J. (2000). An RNA-directed nuclease mediates post-transcriptional gene silencing in *Drosophila* cells. Nature *404*, 293–296.
5. Nykanen, A., Haley, B., and Zamore, P.D. (2001). ATP requirements and small interfering RNA structure in the RNA interference pathway. Cell *107*, 309–321.
6. Martinez, J., Patkaniowska, A., Urlaub, H., Luhrmann, R., and Tuschl, T. (2002). Single-stranded antisense siRNAs guide target RNA cleavage in RNAi. Cell *110*, 563–574.
7. Martinez, J., and Tuschl, T. (2004). RISC is a 5′ phosphomonoester-producing RNA endonuclease. Genes Dev. *18*, 975–980.
8. Chiu, Y.L., and Rana, T.M. (2003). siRNA function in RNAi: a chemical modification analysis. RNA *9*, 1034–1048.
9. Elbashir, S.M., Martinez, J., Patkaniowska, A., Lendeckel, W., and Tuschl, T. (2001). Functional anatomy of siRNAs for mediating efficient RNAi in *Drosophila melanogaster* embryo lysate. EMBO J. *20*, 6877–6888.
10. Hutvagner, G., and Zamore, P.D. (2002). A microRNA in a multiple-turnover RNAi enzyme complex. Science *297*, 2056–2060.
11. Song, J.J., Smith, S.K., Hannon, G.J., and Joshua-Tor, L. (2004). Crystal structure of Argonaute and its implications for RISC slicer activity. Science *305*, 1434–1437.
12. Liu, J., Carmell, M.A., Rivas, F.V., Marsden, C.G., Thomson, J.M., Song, J.J., Hammond, S.M., Joshua-Tor, L., and Hannon, G.J. (2004). Argonaute2 is the catalytic engine of mammalian RNAi. Science *305*, 1437–1441.
13. Meister, G., Landthaler, M., Patkaniowska, A., Dorsett, Y., Teng, G., and Tuschl, T. (2004). Human Argonaute2 mediates RNA cleavage targeted by miRNAs and siRNAs. Mol. Cell *15*, 185–197.
14. Chiu, Y.L., Cao, H., Jacque, J.M., Stevenson, M., and Rana, T.M. (2004). Inhibition of human immunodeficiency virus type 1 replication by RNA interference directed against human transcription elongation factor P-TEFb (CDK9/CyclinT1). J. Virol. *78*, 2517–2529.
15. Zeng, Y., and Cullen, B.R. (2002). RNA interference in human cells is restricted to the cytoplasm. RNA *8*, 855–860.
16. Kawasaki, H., and Taira, K. (2003). Short hairpin type of dsRNAs that are controlled by tRNA(Val) promoter significantly induce RNAi-mediated gene silencing in the cytoplasm of human cells. Nucleic Acids Res. *31*, 700–707.
17. Chiu, Y.L., Ali, A., Chu, C.Y., Cao, H., and Rana, T.M. (2004). Visualizing a correlation between siRNA localization, cellular uptake, and RNAi in living cells. Chem. Biol. *11*, 1165–1175.
18. Schwarz, D.S., Hutvagner, G., Haley, B., and Zamore, P.D. (2002). Evidence that siRNAs function as guides, not primers, in the *Drosophila* and human RNAi pathways. Mol. Cell *10*, 537–548.
19. Clegg, R.M. (2002). FRET tells us about proximities, distances, orientations and dynamic properties. J. Biotechnol. *82*, 177–179.
20. Bastiaens, P.I., Majoul, I.V., Verveer, P.J., Soling, H.D., and Jovin, T.M. (1996). Imaging the intracellular trafficking and state of the AB5 quaternary structure of cholera toxin. EMBO J. *15*, 4246–4253.
21. Kenworthy, A.K., and Edidin, M. (1998). Distribution of a glycosylphosphatidylinositol-anchored protein at the apical surface of MDCK cells examined at a resolution of <100 A using imaging fluorescence resonance energy transfer. J. Cell Biol. *142*, 69–84.
22. Robb, G.B., Brown, K.M., Khurana, J., and Rana, T.M. (2005). Specific and potent RNAi in the nucleus of human cells. Nat. Struct. Mol. Biol. *12*, 133–137.
23. Brown, K.M., Chu, C.Y., and Rana, T.M. (2005). Target accessibility dictates the potency of human RISC. Nat. Struct. Mol. Biol. *12*, 469–470.